Magnets for Low-Emittance Storage Rings an Overview

Pierre Schnizer and Johan Bengtsson

(Invited Paper)

***Abstract*—Low emittance machines require lattices with many magnets of short length. Furthermore, successful lattices require strong gradients with strong dipole fields. These lattices are popular today, as MAX IV has demonstrated that a diffraction limited synchrotron light source can be based on such a lattice. This paper gives an overview of the various magnets used by the various diffraction limited light sources – available, under construction or designed. It compares the different magnet design and technology used and presents the magnet parameters in a consistent fashion.**

***Index Terms*—Conventional magnets, low emittance machines, permanent magnets.**

I. Introduction

LIGHT sources provide X-rays to their users by bending electrons in magnetic fields: i.e. synchrotron radiation. Originally applying X-rays of high energy physics accelerators (as additional users), soon dedicated accelerators were built providing synchrotron light to users. The brightness of X-rays provided to the users could be increased by dedicated insertion devices with magnets that locally wiggle the beam.

Soon the emittance of the accelerator turned out to be limiting the flux. The designers of the MAX IV accelerator showed [1] a light source could reduce the emittance limit by orders of magnitude: the usage of sophisticated combined function magnets lends to a more robust design [2], [3]. The MAX IV performance optimization exploits the balance of the following effects to achieve dynamic emittance equilibrium (see [4]), with a time constant in the order of 10 ms:

1) The electrons emit light in their direction of motion, but are only accelerated in the longitudinal direction. This process reduces the emittance of the electron beam.
2) The magnets – in particular the dipoles – act similar to "mass spectrometers". When electrons radiate, their energy changes, thus their path will be on a "chromatic trajectory". This increases the emittance of the beam.

Electrons dissipate energy and thus lose relativistic mass. The dipoles work as "mass spectrometers" and thus the beam gets larger in the horizontal plane. Therefore the electron beam is much wider in the horizontal plane than in the vertical plane. If uniform identical dipoles are used the optimal emittance ϵ_x is proportional to

$$\epsilon_x \propto \frac{E^2}{N_\mathrm{b}^3} \tag{1}$$

with E the beam energy, N_b the number of dipoles [5].

Accelerators, however, need to correct chromatic aberrations, i.e. that electrons with different energy have different trajectories. These effects are compensated with sextupoles in dispersive regions (i.e. regions where the electrons most deviate from the design orbit if their energy differs from the ideal energy). When these are placed between short dipoles, electrons with energy deviations will be less offset from the ideal orbit, thus the sextupoles strength has to be increased.

Quadrupoles focus the electrons: those whose initial conditions are slightly off axis or with an angle will be kept within limits to the ideal orbit. The electrons maximum deviation (i.e. the dispersion trajectory) from the ideal orbit is rather small for low emittance accelerators. It can be shown that this offset is proportional to $\sqrt{\epsilon_x}$ and hence the quadrupole gradients scale with $1/\epsilon_x$.

As mentioned above: electrons scatter with each other inelastic, thus momentum is transferred from one electron to an other. If this transferred momentum is too large the electron will be lost. The scattering is called *Touschek scattering*; electrons lost cause the beam current to decrease: thus one commonly refers to this effect as *Touschek lifetime*. The number of electrons lost per time unit has to be limited due to radiation protection requirements.

Touschek lifetime scales roughly with the inverse of E^3, therefore this effect is more dominant for accelerators operated at medium energy (∼3 GeV) than for the ones at high (∼6 GeV) energy. Thus especially the magnet lattice of medium energy rings has to be designed in such a manner that larger momentum deviations can be accepted. This is typically achieved by higher order achromats: i.e. electron trajectories will be independent of deviations in position, angle or energy: at least within tolerances.

Point 2, however, can be influenced by proper magnet design and arranging them in a clever manner: by splitting up magnets in many different pieces [1] or combining dipoles and quadrupoles [3] together with introducing anti-bends into the ring [2].

Manuscript received November 30, 2021; revised February 11, 2022 and March 13, 2022; accepted March 14, 2022. Date of publication April 8, 2022; date of current version April 29, 2022. *(Corresponding author: Pierre Schnizer.)*

The authors are with the Helmholtz-Zentrum Berlin für Materialien und Energie, 14109 Berlin, Germany (e-mail: pierre.schnizer@helmholtz-berlin.de).

Color versions of one or more figures in this article are available at https://doi.org/10.1109/TASC.2022.3164033.

Digital Object Identifier 10.1109/TASC.2022.3164033

TABLE I
STATUS, DESIGN CIRCUMFERENCE AND ENERGY OF THE DIFFERENT ACCELERATORS C...MACHINE CIRCUMFERENCE, E...BEAM ENERGY

machine	status	C [m]	E [GeV]
MAX IV	operation	528	3
ESRF-EBS	operation	844	6
Sirius	commissioning	518	3
APS-U	construction	1104	6
Elettra 2.0	funded	259	2
ALS-U	TDR	197	2
SLS-2	TDR	290	2.7
Soleil U	CDR	354	2.75

TABLE II
MAGNETS APERTURES FOR THE DIFFERENT MACHINES: TYPE...MAGNET TYPE, C...MACHINE CIRCUMFERENCE, r_{p} MAGNET GAP OR POLE RADIUS, r_{ref} REFERENCE RADIUS

machine	type	$r_{\mathrm{p}}[mm]$ min	$r_{\mathrm{p}}[mm]$ max	r_{ref} [mm]
MAX IV	all	12.5		10.7
ESRF-EBS	DQ1,DQ2			7
	others	12.6	19.2	13
Sirius	all	27.5		12
APS-U	all	13		10
Elettra 2.0	all	13	16	
ALS-U	all	12	20	5
SLS-2	all	13	20	
Soleil U	all	13	20	5

While damping rings (e.g. for CLIC [6]) solely require to reduce beam's emittance, light sources further require that the beam is stable at each beam spot (i.e. the spot where the X-rays are emitted to the user and thus act as source spot for the users experiment). This is achieved by minimising the vibration of the magnet system including its girders and support structure [7] or actively compensate the impact of the vibrations on the electron beam.

Until the past millenium's end synchrotron light sources were based on an arrangement of dipoles followed by a set of quadrupole doublets or triplets, which provided well controlled beam parameters for the following insertion devices. Sextupoles were used to control the linear chromaticity of the beam. The project MAX IV [1] split up the magnets in many different pieces and miniaturised the aperture of these magnets so that the required field strength of the used quadrupoles and sextupoles could be provided by iron dominated magnets. This design change reduced the emittance of this accelerator by an order of magnitude compared to the emittance that a classical design would achieve.

Successful commissioning of the MAX IV accelerator [1] pushes other projects to pursue the concept of a small periodic structure in the accelerator: ESRF-EBS [8], SIRIUS [9], APS-U [10], HEPS [11], SKIF [12], ALS-U [13], Elettra 2 [14], PETRA IV [15], SLS-2 [16] and Diamond II [17]. Furthermore upgrades are planned for other accelerators e.g. Synchrotron Soleil Upgrade [18], BESSY III [19] AfLS [20] or the Canadian Light Source [21] (see also Table I and Table II). Sirius and ESRF magnet designers started using permanent magnets for their accelerator magnets [8], [22] for their compactness, reliability and energy effectiveness: e.g ESRF reached in that manner that the accelerator is built using identical hot swappable power converters [8]: converters for magnets with dipole or quadrupole components are swapped automatically while higher order correctors can be swapped by the operator.

In this paper, the authors gather available literature material concerning several magnet types from projects of Table I, with a focus on magnets' geometric parameters and performance. In the following sections the available data are presented in a consistent fashion.

The next session presents first an overview of the main field strength of different small aperture accelerator magnets: these are given for the different accelerators next to some information on how these are being built. The different designs of the magnets are mentioned in the text. Their field quality is presented for a reference radius of $r_{\mathrm{ref}} = 10$ mm. First the field quality is presented if only the main coil winding is powered. As far as available the field quality is then reported if added corrector windings are powered.

The distance between the magnets is rather limited for low emittance rings, thus cross talk is expected between them. Measurements have been published. Their findings are summarised in section III.

Magnets need to be aligned with respect to the foreseen ideal orbit. Here different requirements are typically set to the alignment of one magnet to its neighbours, which are usually installed on a common girder. More relaxed alignment requirements are typically made for these girder alignments. Typical number are presented in section IV.

In some accelerators a few arc dipoles are replaced with versions that provide a similar beam deflection but a higher magnetic flux. These magnets are called super bends. Such magnets are reported in section V.

Quite a number of the magnets addressed here are curved: e.g. longitudinal gradient bends or reverse bends. A concise description of the field quality should be based on a coordinate system that follows this curvature. Possible solutions are addressed in section VI.

Section VII covers shortly the performance that was reached by permanent magnets.

The authors intention is that a magnet designer working for the next small emittance ring can use this paper as a first stop of information. It should give first insight which performance magnets reached that have been built for such accelerators or which operation parameters these magnets are being designed for.

II. MAGNETS OVERVIEW

The magnet data presented here are based on results published by the different projects (see Table I). The following projects are completed and are now in operation

- MAX IV: presented data are based on [7].

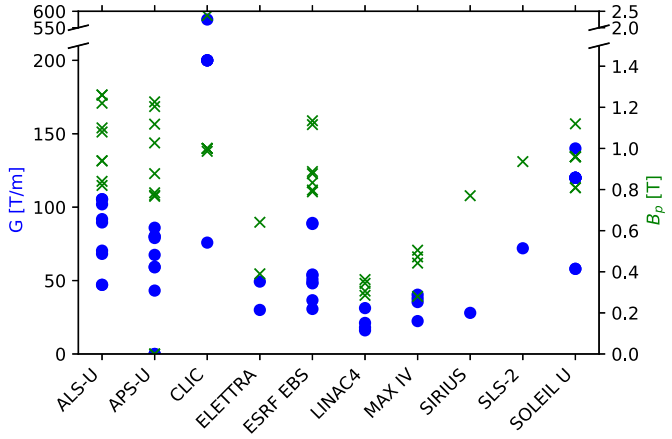

Fig. 1. Gradient and pole tip field for the main quadrupoles for the different machines. The nominal gradients for the different quadrupoles are depicted by blue circles while the pole tip field is indicated by green crosses.

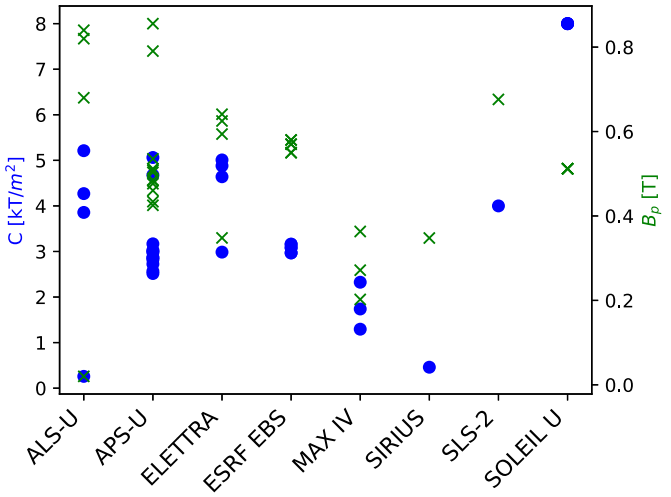

Fig. 2. Strength and pole tip field for the sextupoles for the different projects.

- ESRF-EBS: presented data are based on [8]. A quadrupole using permanent magnets has been designed by the magnet team of this project [23]. Similar designs are now being pursued by SLS-2 or SOLEIL's upgrade project teams.

SIRIUS is currently at the end of its commissioning phase. Magnet data are available at [24]. The project APS-U is currently under construction with many magnets already built; its magnet parameters were extracted from [10]. Measurement data were not available to the authors. The authors are convinced that these will be published at a later stage.

Many projects are currently in their design phase. Different model or prototype magnet were built:

- A reverse bend quadrupole magnet was built for ALS-U [25]. Its magnetic field was measured [26], but no published measurement results were found.
- A quadrupole has been built for the PETRA IV project [15]. Published data were not found by the authors.
- A longitudinal gradient bend magnet was built for SLS-2 [27].

Additionally to the data of the projects mentioned above data are presented for CLIC or LINAC4 magnets. For both projects prototype magnets were built and tested. LINAC4 built and tested quadrupoles based on permanent magnets [28], [29]. CLIC built and tested quadrupoles with a pole radius of 5 mm [30], [31].

A. *Main Field Strength*

The field strength and the pole tip field is presented for quadrupoles in Fig. 1. Different magnets of one machine are depicted on one vertical line. MAX IV, ESRF-EBS and SIRIUS magnets have been built and measured. One can see that rather moderate gradients and pole tip fields were used for MAX IV magnets. The required quadrupole design strength was increased for the following projects (e.g. ESRF-EBS, APS-U and ALS-U). ALS-U is using cobalt based pole shoes for achieving this field strength [13], [26]. The impact of splitting quadrupole pole shoe and return yoke in different pieces is analysed in [32]. Designs with permanent magnets as gradient amplifiers were investigated and evaluated [33]. Sirius quadrupoles are based on this design. Strong gradient were reached by model magnets built and tested for CLIC: 200 T/m were reached for a rather conventional electromagnet design with 5 mm pole radius [30]. A prototype of CLIC's final focus quadrupole was built and tested [31]. It achieved $\approx$ 550 T/m using a Halbach type quadrupole [34] combined with a strong electromagnetic quadrupole. This value is given to show which quadrupole strength could be reached with rather conventional technology; it is assumed that the power requirements of this electromagnet would not be compatible with the energy requirement of a light-source. The values for LINAC 4 quadrupoles were extracted from [35]; quadrupole prototypes using permanent magnets were built and measured [28], [29].

The strength of the different sextupoles is presented in Fig. 2.

All these sextupoles are based on conventional electromagnets. Some of these magnets provide additional windings, which allow using these magnets as corrector magnets too (see also section II-B2). Sextupole main field strength vary (see Fig. 2): similar as for quadrupoles projects seem to build on the achievements demonstrated by already realized ones. MAX IV used rather modest sextupoles strength to achieve design values reliably for their integrated block design [36], [37]. Following projects increase the strength, with ALS-U again heading for highest values.

Octupoles are not used by all light sources. Rather moderate pole tip fields seem to be sufficient for octupoles (see Fig. 3). Their strength is given on the left vertical axis (blue points) while the pole tip field is presented on the right vertical axis (green 'x'). One can see that the requirements of the different machines vary significantly.

Following the proposals of [3] low emittance machines include magnets that combine dipole and quadrupole components within a single magnet. Dipole like – i.e. a gradient was added to some dipole by tilting its pole shoes – were common practise for first strong focusing machines (e.g. [38], [39]). Similar combined function magnets were used for MAX IV and SIRIUS (see Fig. 4). These are also foreseen for ALS-U and SLS-2. CLIC

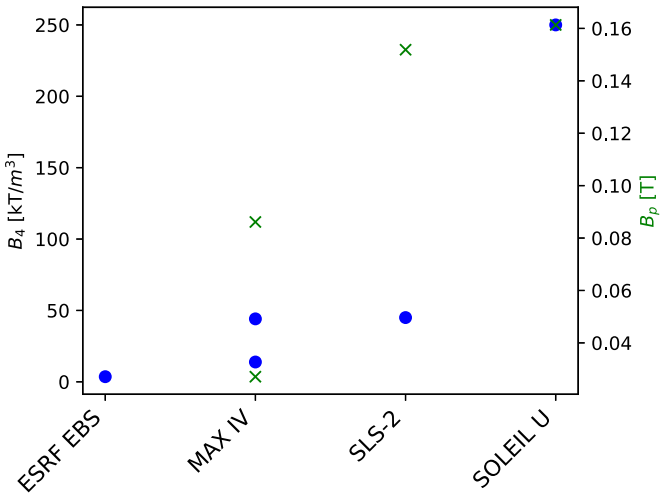

Fig. 3. Gradient and pole field for the octupoles of the different projects.

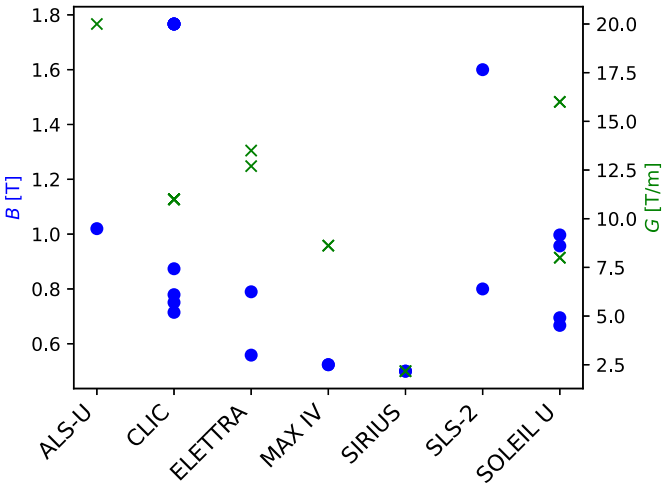

Fig. 4. Combined function magnets: dipole like. Blue circles indicate the dipole field strength (left axis). Green crosses depict the quadrupole gradient strength (right axis).

design values are given here to broaden the view. Please note that many machines use longitudinal gradient bends: these are dipoles with different gaps combined within a common yoke. The dipole strength due to the different gaps is represented in Fig. 4.

ESRF-EBS required dipole components combined with stronger gradients than MAX IV, thus they use a design with 4 poles [40], which is similar to a half quadrupole. Note that the pole shoes are not straight but follow the beam's curvature. Their strength is reflected in Fig. 5. Again ALS-U design is striving for rather strong values [25] using Cobalt-Iron based pole shoes. A prototype magnet was built and measured [26] but data were not yet available to the authors.

B. Field Quality

2D planar complex harmonics are used for describing the magnetic field quality, which is called Beth's representation [41] (a more didactic introduction is found e.g. in [42]–[44]). It is

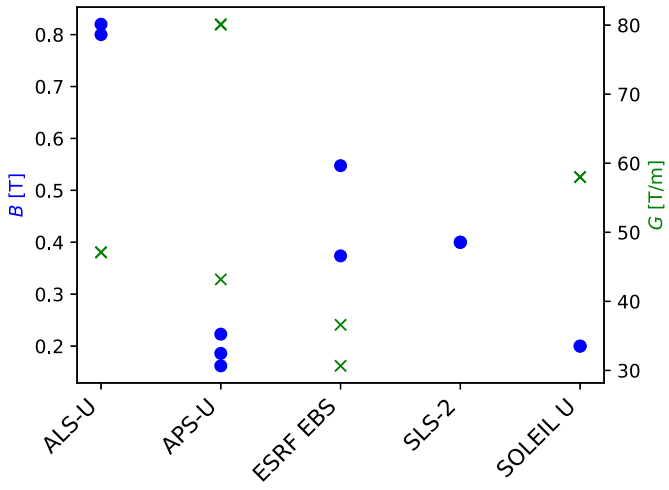

Fig. 5. Combined function magnets: quadrupole like.

given by

$$\mathbf{B}(\mathbf{z}) = B_y(x+\mathtt{i}y) + \mathtt{i}B_x(x+\mathtt{i}y) = \sum_{n=1}^{\infty} \mathbf{C_n} \left(\frac{\mathbf{z}}{r_{\text{ref}}}\right)^{n-1}. \tag{2}$$

for a 2D Cartesian field x, y, $\mathbf{z} = x + \mathtt{i}y$ with the 2D Cartesian magnetic field components B_x, B_y. The complex coefficients $\mathbf{C_n}$ are given by $\mathbf{C_n} = B_n + \mathtt{i}A_n$. B_n are referred to as *normal* components while A_n are called *skew* components. Furthermore normalised harmonics $b_n + \mathtt{i}a_n = \mathbf{c_n} = \mathbf{C_n}/\mathbf{C_m}$ are defined, with m the main harmonic. r_{ref} is the reference radius, which is typically chosen such that its associated circle covers the region of interest and that the b_n's and a_n's are small numbers. Please note that the sum in (2) starts at $n = 1$, which is called "European convention". Except for Sirius and APS-U all machines addressed here use this European convention.

In the following all multipole components are presented as normalised harmonics (b_n or a_n) for a reference radius of 10 mm, thus all data were scaled to this radius using

$$\mathbf{c_n} = \mathbf{c'_n} \left(\frac{r_{\text{ref}}}{r'_{\text{ref}}}\right)^{n-m}, \tag{3}$$

with $\mathbf{c'_n}$ the harmonic for the original reference radius r'_{ref}. Please note that for ALS-U the harmonics had to be scaled from $r'_{\text{ref}} = 5$ mm to the larger r_{ref} of 10 mm (see Table I), which is typically problematic.

1) Powered by Main Coil: For the different quadrupoles the higher order harmonics are given in Fig. 6. For MAX IV and ESRF-EBS, the variation of the harmonics due to production is given in [7]. The mean value of each harmonics is represented by the centre cross while its variation is indicated as error bar. For the other machines only reference data were found. Similarly the production variation of the expected harmonics of the sextupoles were only available for MAX-IV (see Fig 7). In this figure, the harmonics are presented when only the main coil is powered and no current is applied to the corrector coil windings.

2) Corrector's Induced Field Quality Deterioration: For synchrotron light sources corrector magnets are typically implemented as corrector windings, which are mounted as additional coil packs on sextupoles or quadrupoles. SIRIUS and ALS-U

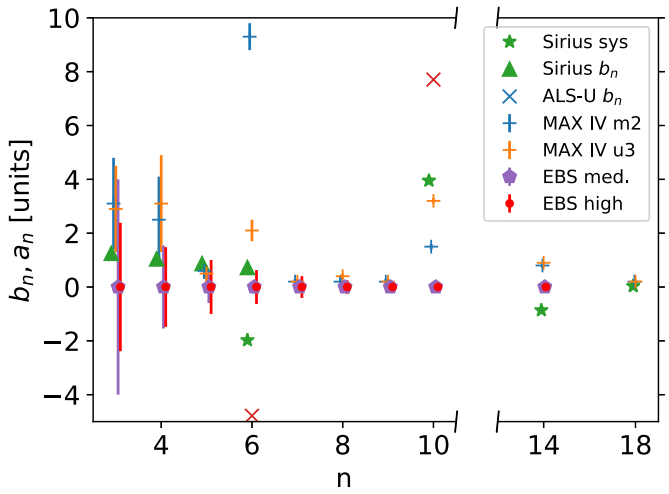

Fig. 6. Higher order harmonics of the quadrupoles. Sirius: sys refers to the allowed harmonics while b_n to additional ones due to manufacturing tolerances. The label 'EBS' refers to ESRF-EBS. *EBS high* refers to quadrupoles, which are operated at roughly 90 T/m. .

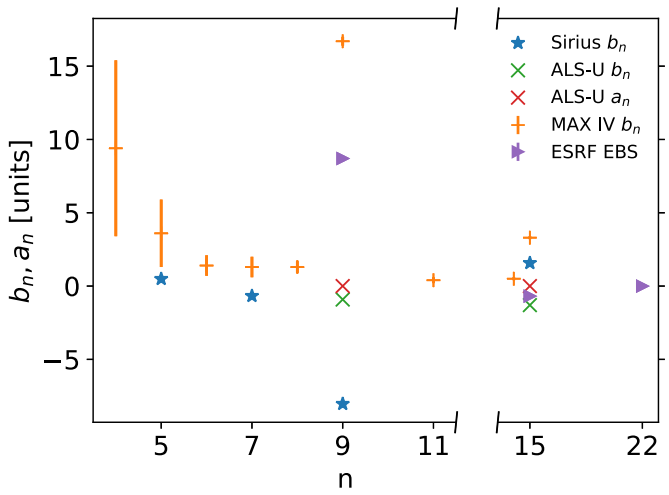

Fig. 7. Higher order harmonics for the sextupoles when only the main coil is powered (correctors off). Nominal multipoles are given for the sextupoles for all machines except for MAX IV: For MAX IV the production variance is indicated as error bar while the mean values are represented by the centre of the error bar.

published data of higher order multipoles as produced by the corrector windings mounted on their quadrupoles (see Fig. 8). and sextupoles (see Fig. 9). These projects published data for more than one magnet type. Thus more than one marker can be given for one harmonic. The higher order harmonics created by the corrector coils are of similar magnitude as the harmonics created by the magnet if the corrector coils are off (compare Fig. 6 to Fig. 8 and compare Fig. 7 to Fig. 9).

The values of the harmonics seem to be rather large: but these are presented for a reference radius of $r_{\mathrm{ref}} = 10$ mm. This covers a significant fraction of the mechanical aperture (see Table II). Furthermore the electron beam diameters are typically well below 50 μm (at 1 σ).

III. Magnet Cross Talk

A low emittance machine requires many magnets, therefore these are assembled with a small gap between them (roughly

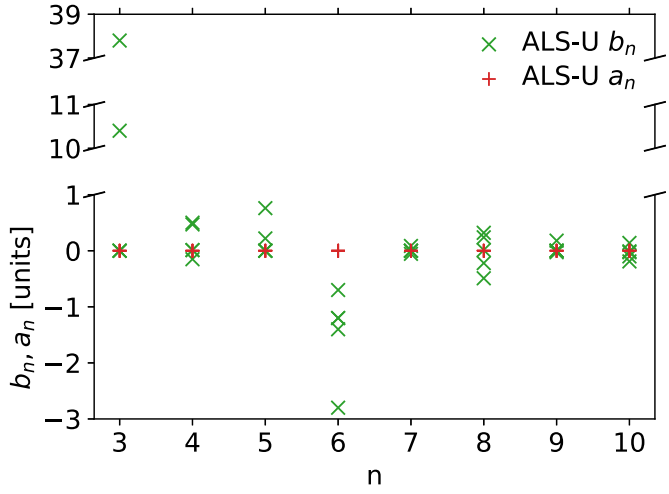

Fig. 8. ALS-U: higher order harmonics of the quadrupoles when the corrector coil is powered.

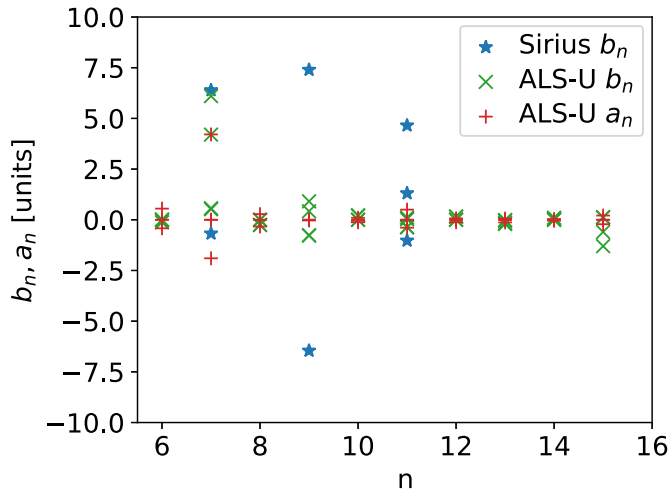

Fig. 9. Higher order harmonics of the sextupole when the corrector coil is powered.

four times the aperture). Therefore cross talk between these magnets is expected (e.g. APS [45], ESS [46]). ESRF-EBS published measurement data [47]. These data show that cross talk is changing the main field component by up to $\approx 2\%$. Calculations were conducted which show that cross talks can be predicted fairly precisely to $\approx 0.03\%$. So future projects are well advised to use appropriate simulation tools for predicting the effect of cross talk. Furthermore these calculations should be qualified by appropriate measurements.

IV. Assembly and Alignment

The small magnets size requires precise machining of the individual pieces the magnets are made of. Here overall tolerances are listed that the different projects require for either manufacturing or alignment tolerances of the different magnets or magnet systems. These should not be confused with the mechanical tolerances for a single magnet subcomponent: e.g. a pole shoe.

The authors refrained to compare the different values within a table, as each project has a slightly different convention. Thus

they considered such a table as misleading. The values listed below are intended to give an overview of typical target values for the different assembly and alignment tasks.

A. Magnet Assembly

MAX IV designed magnets as block assemblies to minimize the impact of mechanical vibrations on the beam and to aggregate components within a single unit [36], [37]. Different papers report that its magnets surfaces were made with an accuracy of $\pm 20 \mu m$ [36], [48], [49]. The magnetic axis of the different magnets was measured with a rotating coil probe. These measurements showed that the axis would vary by less than $< 10\,\mu m$ (root mean square error).

For ESRF-EBS a manufacturing tolerance of $\pm\,20\,\mu m$ is reported for the prototype, which was released to $\pm\,40\,\mu m$ for series production [50], [51].

1) Magnet Alignment: The values listed here apply to transverse alignment. The longitudinal requirements are typically relaxed by an order of magnitude. For magnet alignment ESRF-EBS specified fiducialisation errors to $\pm$ 50 μm. Magnet centres were positioned within $\pm$ 50 μm by mechanical shims. The roll angle of the magnets was initially set to $\pm$ 50 μrad; this value was relaxed to $\pm$ 130 μrad for production (see [52], which also gives a good overview over magnet production).

Petra IV lists targets of 20 - 30 μm for magnet to magnet and magnet to girder alignment while girder to girder alignment is specified to 100 μm [15]. The ALS-U project demands a challenging alignment accuracy of $\pm\,20\,\mu m$ [26].

When comparing alignment of different machines, one should take into account that MAX IV assembled the different magnets within a common block. Thus the tolerances listed for MAX IV in section IV-A should be compared to the tolerances other projects specify for aligning magnets on a common girder.

V. Superbends

Superbends allow providing users with synchrotron radiation at a higher peak than the average dipole provides: e.g. ALS operated such magnets [53], [54] and BESSY II built and tested a 9 Tesla superbend [55].

Today low emittance machines integrate superbends based on permanent magnets e.g. SIRUS [56], which provides a field of $\approx$ 3.2 T. For SLS-2 4 - 6 T superbends are being looked into [57], [58], which are using superconducting coils. Design evaluations were made for superbends based on pole shoes made of Holmium, which are driven by a superconducting coil [59].

VI. On Curvature

Accelerator magnets are typically modelled as thin lenses. Following Beth's approach [60], their field is typically described using 2D complex multipoles (see e.g. [43]).

Within dipoles, longitudinal gradient bends and reverse bends the particle's trajectory is following a circle segment. Thus these magnets are typically curved to minimise their sagitta with respect to the ideal orbit (e.g. [40]).

Typically the aspect ratio $\varepsilon = r_{\mathrm{ref}}/R_{\mathrm{C}}$ allows distinguishing between the different methods. R_{C} is the osculating circle to the beam trajectory within a dipole. If ε is small (for accelerators typically in the order of a per mille or less) local toroidal coordinates allow describing the field [44]. For all aspect ratios global toroidal coordinates allow describing the magnetic field in a manner that follows the curvature of the field e.g. [61]–[64]. Please note, that the expansion is then not necessarily around the magnet's centre. A further option is to develop the field using cylindrical coordinates centred on the "vertical revolution axis," thus using more or less the centre of the ring as reference point (e.g. [65]–[67]). It is expected that these multipoles are correlated, therefore regularisation could be required for a more robust set of coefficients (e.g. [68]–[71]).

For synchrotron light sources local toroidal multipoles could be a good start, even if this is an obviously biased opinion [44].

VII. Permanent Magnets: Achievable Performance

Permanent magnets allowed reducing the size of electrical machinery (e.g. [72]) and have been used for undulators (e.g. [73], [74]) and accelerator magnets (e.g. [75], [76]). Temperature compensation was already addressed then (e.g. [77]–[79]). Long term drifts in the range of 0.04 % were reported [80].

ESRF-EBS is using permanent magnets for the longitudinal gradient bends [50] and has looked into a high gradient magnet based on permanent magnets [23].

Halbach arranged permanent magnets in sectors to amplify the reachable field strength [34]. His ideas have lead to different designs e.g. [81]. Based on this Halbach design different demonstrators have been built. For an aperture of 2 mm a dipole field above 5 T was achieved [82]. Similarly a quadrupole was built with an aperture of 7 mm radius that achieved a gradient of $\approx$ 300 T/m at [83].

The field quality of such Halbach arrays can be limited by the "block design" due to the permanent magnet blocks. CESR showed that the field quality can be significantly improved by shimming the magnets with an insert containing ferromagnetic rods [84].

Permanent magnets are considered to allow minimising the magnets themselves next to the gaps between them and thus minimising the emittance of synchrotron light sources [85] e.g. as no coil packs are required. Overviews are given for permanent magnets e.g. in [86] and for quadrupoles in [87].

VIII. Conclusion

Low emittance machines are nowadays the basis of recently commissioned, currently being constructed or designed synchrotron light sources. The design of the lattice next to their magnets allows reducing the beam emittance of these machines to small values.

This paper compared the field strength and field quality for the different magnets. Dipole fields of 0.8 - 1.8 T are typically used; these are provided by combined function magnets (see Figs. 4 and 5). Quadrupole gradients are in the range from 20 - 100 T/m with pole tip fields in the range of $\approx$ 0.4 - 1.2 T (see Fig. 1). Sextupoles values range from less than 1000 to more than 5000 T/m^2 with a pole tip field up to $\approx$ ˜0.8 T (see Fig. 2).

Multipoles are typically reported as 2D planar relative harmonics following the "European" convention (see (2)). These relative harmonics are typically given in units (1 unit = 100 ppm). Reference radii of 5 to 13 mm are common practise for the listed machines (see Table II). The multipoles of the magnets of the different machines were rescaled to a reference radius of $r_{\mathrm{ref}} = 10$ mm. One can see that the multipoles are in the order of a few units (see Fig. 6 and Fig. 7). Correctors mounted on sextupoles (for ALS-U also on quadrupoles) produce not-allowed harmonics of similar strength as the allowed ones of the main magnet (see Figs. 8 and 9).

Accelerator magnets were based on permanent magnets since Fermilab's recycler [75]. ESRF-EBS uses permanent magnets for longitudinal gradient bends. For quadrupole magnets different designs were made which are using permanent magnets instead of coils or permanent magnets are used as gradient amplifiers additionally to conventional coil packs. These designs uses partly pole shoes made of CoFe material. Highest gradients were achieved for apertures of a few millimetres with magnets based on Halbach arrays. The CESR project achieved accelerator grade field quality for Halbach array based magnets using a shimming method based on small ferromagnetic rods.

Two light sources based on the multibend achromat design were built with many others being under construction or being designed. The key performance parameters of their accelerator magnets were reported here. Future will show in which direction the magnet design will evolve for storage ring based light sources.

REFERENCES

[1] N. Martensson and M. Eriksson, "The saga of MAX IV, the first multi-bend achromat synchrotron light source," *Nucl. Instrum. Meth. Phys. Res. Sect. A*, vol. 907, pp. 97–104, 2018.

[2] A. Streun, "The anti-bend cell for ultralow emittance storage ring lattices," *Nucl. Instrum. Meth. Phys. Res. Sect. A*, vol. 737, pp. 148–154, 2014.

[3] S. C. Leemann and A. Streun, "Perspectives for future light source lattices incorporating yet uncommon magnets," *Phys. Rev. ST Accel. Beams*, vol. 14, Mar. 2011, Art. no. 030701.

[4] A. Wolski, "Low-emittance storage rings," pp. 245-294. 50 p, Jul 2015, presented at the CERN Accel. School CAS 2013: *Adv. Accel. Phys. Course*, Trondheim, Norway, 18–29 Aug. 2013.

[5] L. Teng, "Minimum emittance lattice for synchrotron radiation storage rings," *Argonne Nat. Lab.*, Tech. Rep. LS-17, Mar. 1985. [Online]. Available: https://www.aps.anl.gov/files/APS-sync/lsnotes/files/APS_1417575.pdf

[6] M. Aicheler *et al.*, "A multi-TeV linear collider based on CLIC technology, CLIC conceptual Des. Rep.," CERN Eur. Org. Nucl. Res., Tech. Rep. CERN-2012-007, 2021.

[7] F. Bødker, C. Hansen, D. Kristoffersen, L. Baandrup, C. Ostenfeld, and C. Pedersen, "Mechanical and magnetic performance of compact synchrotron magnet systems for MAX IV and SOLARIS," in *Proc. IPAC2014*, 2014, pp. 1229–1231.

[8] P. Raimondi and D. Einfeld, Eds., "ESRF – EBS design report," ESRF, Tech. Rep., Sep. 2018. [Online]. Available: https://www.esrf.fr/files/live/sites/www/files/about/upgrade/documentation/Design%20Reportreduced-jan19.pdf

[9] L. Liu, R. T. Neuenschwander, and A. R. D. Rodrigues, "Synchrotron radiation sources in Brazil," *Philos. Trans. Roy. Soc. A.*, vol. 377, no. 2147, pp. 1–9, 2019.

[10] T. Fornek "Advanced photon source upgrade project, final design report" Argonne Nat. Lab., Tech. Rep. APSU-2.01-RPT-003, May 2019, doi: 10.2172/1543138.

[11] Y. Jiao *et al.*, "The HEPS project," *J. Synchrotron Radiat.*, vol. 25, no. 6, pp. 1611–1618, Nov. 2018.

[12] G. Baranov, A. Bogomyagkov, E. Levichev, and S. Sinyatkin, "Lattice optimization of the Novosibirsk fourth-generation light source Skif," 2021, *arXiv:2107.03081*.

[13] "Advanced light source upgrade project. conceptual design report," Lawrence Berkeley Nat. Lab., Tech. Rep., Jun. 2018.

[14] E. Karantzoulis *et al.*, "Elettra 2.0 technical conceptual design report," Elettra - Sincrotrone Trieste, Tech. Rep. ST/M-17/01, 2017.

[15] C. G. Schroer *et al.*, "PETRA IV, upgrade of PETRA III to the ultimate 3D x-ray microscope conceptual design report," DESY, *Tech. Rep.*, 2019, doi: 10.3204/PUBDB-2019-03613.

[16] A. Streun *et al.*, "SLS-2 conceptual design report," Paul Scherrer Institut, Tech. Rep., (PSI Bericht, Report No.: 17-03), Dec. 2017. [Online]. Available: https://www.dora.lib4ri.ch/psi/islandora/object/psi:34977

[17] L. Chapon *et al.*, "Diamond-II, conceptual design report," *Diamond Light Source Ltd., Tech. Rep.*, May 2019. [Online]. Available: https://www.diamond.ac.uk/dam/jcr:ec67b7e1-fb91-4a65-b1cef646490b564d/Diamond-II%20Conceptual%20Design%20Report.pdf

[18] "Synchrotron soleil upgrade, conceptual design report," SYNCHROTRON SOLEIL, Tech. Rep., 2021. [Online]. Available: https://www.synchrotron-soleil.fr/en/file/13803/download?token=OUzsp46P

[19] P. Goslawski *et al.*, "BESSY III & MLS II - status of the development of the new photon science facility in berlin," in *Proc. 12th Int. Part. Acc. Conf. IPAC2021, Campinas, SP*, 2021, pp. 451–454.

[20] "Conceptual Design Report Afrikan Light Source." Accessed: Feb. 2, 2022. [Online]. Available: https://www.africanlightsource.org/afls-roadmap-cdr/

[21] L. Dallin and W. Wurtz, "Towards a 4th generation storage ring at the Canadian Light Source," *AIP Conf. Proc.*, vol. 1741, no. 1, 2016, Art. no. 020034.

[22] J. Citadini *et al.*, "Sirius–a 3GeV electron storage ring based on permanent magnets," *IEEE Trans. Appl. Supercond.*, vol. 22, no. 3, Mar. 2012, Art. no. 4004404.

[23] P. N'gotta, G. Le Bec, and J. Chavanne, "Hybrid high gradient permanent magnet quadrupole," *Phys. Rev. Accel. Beams*, vol. 19, Dec. 2016, Art. no. 122401.

[24] Sirius Light Source Wiki Entry, Sep. 2018. Accessed: Nov. 21, 2021. [Online]. Available: https://wiki-sirius.lnls.br/mediawiki/index.php?title=Machine:Magnets&oldid=7142

[25] J. Y. Jung *et al.*, "Design of asymmetric quadrupole gradient bending r&d magnet for the advanced light source upgrade (ALS-U)," in *Proc. 9th Int. Part. Accel. Conf. IPAC2018*, 2018, pp. 3667–3669.

[26] E. Wallén, C. Wouters, R. Teyber, and L. Fajardo, "Magnetic measurements for the ALS-U," Presented at Int. Magnetic Meas. Workshop, IMMW 21, 2019. [Online]. Available: https://www.esrf.fr/files/live/sites/www/files/events/conferences/2019/IMMW21/presentationEventManager/Wallen_IMMW21.pdf

[27] C. Calzolaio *et al.*, "Longitudinal gradient bend magnets for the upgrade of the Swiss Light Source storage ring," *IEEE Trans. Appl. Supercond.*, vol. 30, no. 4, Feb. 2020, Art. no. 8993715.

[28] D. Tommasini, M. Buzio, P. A. Thonet, and A. Vorozhtsov, "Design, manufacture and measurements of permanent quadrupole magnets for Linac4," *IEEE Trans. Appl. Supercond.*, vol. 22, no. 3, Dec. 2012, Art. no. 4000704.

[29] M. Buzio, G. Golluccio, A. Lombardi, and F. Mateo, "Magnetic qualification of permanent magnet quadrupoles for CERN's Linac4," *IEEE Trans. Appl. Supercond.*, vol. 22, no. 3, Mar. 2012, Art. no. 4004304.

[30] M. Modena and C. Petrone, "Performance of the optimized mechanical design of the CLIC main-beam quadrupole magnet prototype," *IEEE Trans. Appl. Supercond.*, vol. 30, no. 4, Feb. 2020, Art. no. 4001505.

[31] M. Modena *et al.*, "Design, assembly and first measurements of a short model for CLIC final focus hybrid quadrupole QD0," in *Proc. IPAC2012*, 2012, pp. 3515–3517.

[32] J. Liu, R. Dejus, A. Donnelly, C. Doose, A. Jain, and M. Jaski, "Field quality from tolerance analyses in eight-piece quadrupole magnet," *IEEE Trans. Appl. Supercond.*, vol. 28, no. 3, Nov. 2018, Art. no. 4001104.

[33] G. Tosin, P. Palma Sanchez, J. F. Citadini, and C. Castro Vergasta, "Super hybrid quadrupoles," *Nucl. Instrum. Meth. Phys. Res. Sect. A*, vol. 674, pp. 67–73, 2012.

[34] K. Halbach, "Application of permanent magnets in accelerators and electron storage rings (invited)," *J. Appl. Phys.*, vol. 57, no. 8, pp. 3605–3608, 1985.

[35] L. Arnaoudon *et al.*, "Linac4 technical design report," CERN Tech. Rep. CERN-AB-2006-084, 2006. [Online]. Available: https://cds.cern.ch/record/1004186

[36] M. Johansson, B. Anderberg, and L.-J. Lindgren, "Magnet design for a low-emittance storage ring," *J Synchrotron Radiat.*, vol. 21, no. 5, pp. 884–903, Sep. 2014.

[37] D. Einfeld and M. Johansson, "Magnets for MAX IV," *Presented At 3rd Low Emittance Workshop*, Oxford, United Kingdom, Jul. 2013. [Online]. Available: https://indico.cern.ch/event/247069/contributions/1568406/

[38] E. Regenstreif, Ed., The CERN Proton Synchrotron, ser, CERN Yellow Reports: Monographs. Geneva: CERN, Tech. Rep. CERN-62-03, 1959, ch. 3, [Online]. Available: https://cds.cern.ch/record/214352

[39] J.-P. Burnet *et al.*, "Fifty years of the CERN Proton Synchrotron: Volume 1," ser. CERN Yellow Reports: Monographs. Geneva: CERN, Eur. Org. Nucl. Res., Tech Rep. CERN-2012-007, 2021, ch. 2, pp. 33–49. [Online]. Available: https://cds.cern.ch/record/1359959

[40] G. Le Bec, S. Liuzzo, F. Villar, P. Raimondi, and J. Chavanne, "Single sided dipole-quadrupole magnet for the Extremely Brilliant Source storage ring at the European Synchrotron Radiation Facility," *Phys. Rev. Accel. Beams*, vol. 22, Oct. 2019, Art. no. 102402.

[41] R. A. Beth, "Complex representation and computation of two-dimensional magnetic fields," *J. Appl. Phys.*, vol. 37, no. 7, pp. 2568–2571, 1966.

[42] A. K. Jain, "Basic Theory of Magnets," *CAS Meas. and Alignment*, S. Turner, Ed CERN, Aug. 1998, pp. 1–21.

[43] A. Wolski, "Maxwell's equations for magnets," in *CERN Accel. : Specialised Course on Magnets*, D. Brandt, Ed., vol. CERN-2010-004, CERN., 2010, pp. 1–38, *published as CERN Yellow Report* http://cdsweb.cern.ch/record/1158462

[44] P. Schnizer, *Multipoles for Magnets, and Their*. Springer, 2017.

[45] M. Abliz, M. Jaski, A. Jain, M. Borland, G. Decker, and J. Kerby, "Magnetic cross-talk simulation between Q2 and L-bend magnets of APS-U," *Nucl. Instrum. Meth. Phys. Res. Sect. A*, vol. 913, pp. 48–53, 2019.

[46] D. Fernández-Cañto, J. Muñz, I. Rueda, and I. Bustinduy, "Magnetic analysis and cross-talk fields for the ESS MEBT quadrupole magnet," *Nucl. Instrum. Meth. Phys. Res. Sect.*, vol. 1014, 2021, Art. no. 165723.

[47] G. Le Bec, J. Chavanne, S. Liuzzo, and S. White, "Cross talks between storage ring magnets at the Extremely Brilliant Source at the European Synchrotron Radiation Facility," *Phys. Rev. Accel. Beams*, vol. 24, Jul. 2021, Art. no. 072401.

[48] J. Björklund Svensson and M. Johansson, "Relative alignment within the MAX IV 3GeV storage ringmagnet blocks," in *Proc. 6th Int. Part. Accel. Conf., IPAC2015*, 2015, pp. 57–59.

[49] M. Johansson, L.-J. Lindgren, M. Sjöström, and P. F. Tavares, "MAX IV 3GeV storage ring magnet block production series measurement results," in *Proc. IPAC2016*, Busan, Korea, 2016, Art. no. 1157.

[50] G. Le Bec *et al.*, "Magnets for the ESRF diffraction-limited light source project," *IEEE Trans. Appl. Supercond.*, vol. 26, no. 4, pp. 1–8, Dec. 2016.

[51] C. Benabderrahmane *et al.*, "Magnets for the ESRF-EBS project," in *Proc. IPAC2016*, 2016, pp. 1096–1099.

[52] G. Le Bec, L. Lefebvre, C. Penel, and J. Chavanne, "Measurement and fiducialization of the ESRF-EBS magnets," *Presented at Int. Magn. Meas. Workshop*, IMMW 21, 2019. [Online]. Available: https://www.esrf.fr/files/live/sites/www/files/events/conferences/2019/IMMW21/presentationEventManager/IMMW21%20--%20LeBec%20--%20EBS%20Meas.pdf

[53] S. Marks *et al.*, "ALS superbend magnet performance," *IEEE Trans. Appl. Supercond.*, vol. 12, no. 1, pp. 149–152, Aug. 2002.

[54] D. Robin, "Superbend upgrade at the advanced light source," in *Proc. the 2003 Part. Accel. Conf.*, 2003, pp. 224–228.

[55] A. Batrakov *et al.*, "Nine tesla superconducting bending magnet for BESSY-II," *Nucl. Instrum. Meth. Phys. Res. Sect. A*, vol. 543, no. 1, pp. 35–41, 2005.

[56] J. Citadini, L. N. P. Vilela, R. Basilio, and M. Potye, "Sirius: Details of the new 3.2 T permanent magnet Superbend," *IEEE Trans. Appl. Supercond.*, vol. 28, no. 3, Dec. 2018, Art. no. 4101104.

[57] C. Calzolaio, S. Sanfilippo, S. Sidorov, A. Anghel, and A. Streun, "Design of a superconducting longitudinal gradient bend magnet for the SLS upgrade," *IEEE Trans. Appl. Supercond.*, vol. 27, no. 4, pp. 1–5, Nov. 2017.

[58] C. Calzolaio, G. Montenero, and S. Sanfilippo, "Superconducting longitudinal gradient bend for the Swiss Light Source upgrade: Thermo-mechanical study," *IEEE Trans. Appl. Supercond.*, vol. 29, no. 5, Feb. 2019, Art. no. 4101204.

[59] M. Juchno *et al.*,, "Conceptual design of superbend and hardbend magnets for advance light source upgrade project," *IEEE Trans. Appl. Supercond.*, vol. 30, no. 4, Jan. 2020, Art. no. 4100505.

[60] R. A. Beth, "Complex representation and computation of two-dimensional magnetic fields," *Appl. Phys.*, vol. 37, pp. 2568–71, 1966.

[61] P. Moon and D. E. Spencer, *Field Theory Handbook: Including Coordinate, and Their Solutions*. Springer, 1988.

[62] L. Brouwer, S. Caspi, D. Robin, and W. Wan, "3D toroidal field multipoles for curved accelerator magnets," in *Proc. PAC2013*, 2013, pp. 907–909.

[63] L. N. Brouwer, " Canted-cosine-Theta superconducting accelerator magnets for high energy physics and ion beam cancer therapy," Ph.D. dissertation, Univ. California, Berkeley, Tech. Rep. CERN-ACC-2016-0017, Nov. 2016. [Online]. Available: https://cds.cern.ch/record/2132847

[64] D. Veres, T. Vaszary, E. Benedetto, and D. Barna, "A new algorithm for optimizing the field quality of curved CCT magnets," *IEEE Trans. Appl. Supercon. to be submitted*, doi: 10.1109/TASC.2022.3162389.

[65] E. M. McMillan, "Multipoles in cylindrical coordinates," *Nucl. Instrum. Meth.*, vol. 127, no. 3, pp. 471–474, 1975.

[66] S. Mane, "Solutions of Laplace's equation in two dimensions with a curved longitudinal axis," *Nucl. Instrum. Meth. Phys. Res. Sect. A*, vol. 321, no. 1, pp. 365–375, 1992.

[67] T. Zolkin, "Sector magnets or transverse electromagnetic fields in cylindrical coordinates," *Phys. Rev. Accel. Beams*, vol. 20, Apr. 2017, Art. no. 043501.

[68] A. N. Tikhonov, "On the stability of inverse problems," *Doklady Akademii Nauk SSSR*, vol. 39, no. 5, pp. 195–198, 1943.

[69] H. A. E. and R. Kennard, "Ridge regression: Biased estimation for nonorthogonal problems," *Technometrics*, vol. 12, pp. 55–67, 1970.

[70] S. S. Chen, D. D., and M. Saunders, "Atomic decomposition by basis pursuit," *SIAM J. Comp.*, vol. 20, pp. 33–61, 1998.

[71] B. Efron, T. Hastie, I. Johnstone, and R. Tibshirani, "Least angle regression (with discussion)," *Ann. Statist.*, vol. 32, no. 2, pp. 407–409, 2004.

[72] T. Taylor, "Magnets in accelerators: An historical overview," *Presented At the EuCARD-2 XBEAM-XRING Network Beam Dynamics Meets Magnets Workshop*, Darmstadt, Dec. 2013. [Online]. Available: https://indico.gsi.de/event/2352/contributions/8291/

[73] H. Motz, W. Thon, and R. N. Whitehurst, "Experiments on radiation by fast electron beams," *J. Appl. Phys.*, vol. 24, no. 7, pp. 826–833, 1953.

[74] J. Bahrdt and E. Gluskin, "Cryogenic permanent magnet and superconducting undulators," *Nucl. Instrum. Meth. Phys. Res. A*, vol. 907, pp. 149–168, 2018.

[75] G. Foster *et al.*, "Permanent magnet design for the Fermilab main injector recycler ring," in *Proc. Part. Accel. Conf.*, 1995, pp. 1298–1300.

[76] H. Glass *et al.*, "Permanent gradient magnets for the 8GeV transfer line at FNAL," in *Proc. 1997 Part. Accel. Conf.*, 1997, pp. 3263–3265.

[77] K. Bertsche, J.-F. Ostiguy, and W. Foster, "Temperature considerations in the design of a permanent magnet storage ring," in *Proc. Part. Accel. Conf.*, 1995, vol. 2, pp. 1381–1383.

[78] S. Kim and C. Doose, "Temperature compensation of NdFeB permanent magnets," in *Proc. 1997 Part. Accel. Conf.*, 1997, pp. 3227–3229.

[79] R. Schlueter, S. Marks, C. Loper, and K. Halbach, "Temperature compensation in hybrid magnets with application to the Fermilab stacker and recycler ring dipole design," *IEEE Trans. Magn.*, vol. 32, no. 4, pp. 2203–2205, Jul. 1996.

[80] J. T. Volk, "Experiences with permanent magnets at the Fermilab recycler ring," *J. Instrum.*, vol. 6, no. 8, Aug. 2011, Art. no. T08003.

[81] B. Zhang and G. P. Hatch, "Field analysis and comparison of several permanent magnet dipole structures," *IEEE Trans. Magn.*, vol. 45, no. 10, pp. 4395–4398, Sep. 2009.

[82] M. Kumada, E. Antokhin, Y. Iwashita, M. Aoki, and E. Sugiyama, "Super strong permanent dipole magnet," *IEEE Trans. Appl. Supercond.*, vol. 14, no. 2, pp. 1287–1289, Aug. 2004.

[83] T. Mihara, Y. Iwashita, M. Kumada, A. Evgeny, and C. M. Spencer, "Super strong permanent magnet quadrupole for a linear collider," *IEEE Trans. Appl. Supercond.*, vol. 14, no. 2, pp. 469–472, Aug. 2004.

[84] S. Brooks, G. Mahler, J. Cintorino, J. Tuozzolo, and R. Michnoff, "Permanent magnets for the return loop of the Cornell-Brookhaven energy recovery linac test accelerator," *Phys. Rev. Accel. Beams*, vol. 23, Nov. 2020, Art. no. 112401.

[85] P. F. Tavares, J. Bengtsson, and A. Andersson, "Future development plans for the MAX IV light source: Pushing further towards higher brightness and coherence," *J. Electron Spectrosc. Related Phenomena*, vol. 224, pp. 8–16, 2018.

[86] J. Chavanne and G. Le Bec, "Propects for the use of permanent magnets in future accelerator facilities," in *Proc. 5th Int. Part. Accel. Conf.*, 2014, Art. no. 14.

[87] A. Ghaith, D. Oumbarek, C. Kitégi, M. Valléau, F. Marteau, and M.-E. Couprie, "Permanent magnet-based quadrupoles for plasma acceleration sources," *Instrum.*, vol. 3, no. 2, 2019, Art. no. 27, doi: 10.3390/instruments3020027.